E-Plane Forked Hybrid-T Junction*

W. K. KAHN†

Summary—**A novel rearrangement of the waveguides of a microwave hybrid-T junction has been investigated. This junction is formed by the intersection of four rectangular waveguides, two of which (conventionally *E* and *H* arms) are mutually perpendicular, cross-polarized, and have their centerlines in one symmetry plane of the junction; the remaining two waveguide arms are formed by symmetric *E*-plane bifurcation of the *E*-arm waveguide extended. This hybrid T possesses special advantages with regard to match and pulse power capacity.**

A special test fixture was constructed of 1.122-×0.497-inch rectangular waveguide. Experimental design work was carried out over a 12 per cent range of frequencies from 8.5 to 9.6 kmc. The *H*-arm reflection was reduced to 2.6-db standing-wave ratio (swr) by simple shaping of the bifurcating element. Addition of conventional matching elements resulted in maximum reflections, within the above band, of 0.8 and 0.6 db swr in the *H* and *E* arms, respectively.

The ultimate limitation on the *E*-arm power capacity, as fixed by the intensified electric field at the leading (rounded) edge of the center partition, was computed to be 2 db below uniform waveguide. Experimental corroboration has been obtained.

Introduction

THIS PAPER describes the development of a new hybrid-T junction, the *E*-plane forked hybrid-T, for the band from 8.5 to 9.6 kmc. Such junctions prove useful in a variety of microwave measurements and also in some duplexer arrangements where, in addition, high power carrying capacity is required. In the presentation, the particular structure involved will be clarified by exhibiting its relation to the conventional hybrid-T. Then the properties of hybrid-T junctions will be reviewed briefly and incorporated in what is believed to be a new equivalent circuit. The general problem of matching such a junction is discussed in order to point up the special advantage of the *E*-plane forked hybrid-T. The evolution of each of the matching elements and their performance will be indicated. Finally, the inherent power capacity of the *E*-arm of the junction will be estimated on the basis of a simple conformal mapping, and the result compared with experimental data.

Three hybrid-T structures are shown in Fig. 1. The most important feature which these four-ports have in common is a particular type of symmetry with respect to the indicated plane. Two arms, denoted symmetrical arms (ports 1 and 2), are mirror images of each other in the symmetry plane. The remaining two arms (ports 3 and 4) have their centerlines in the symmetry plane *and are cross-polarized.* These are denoted *H* and *E*-arms,

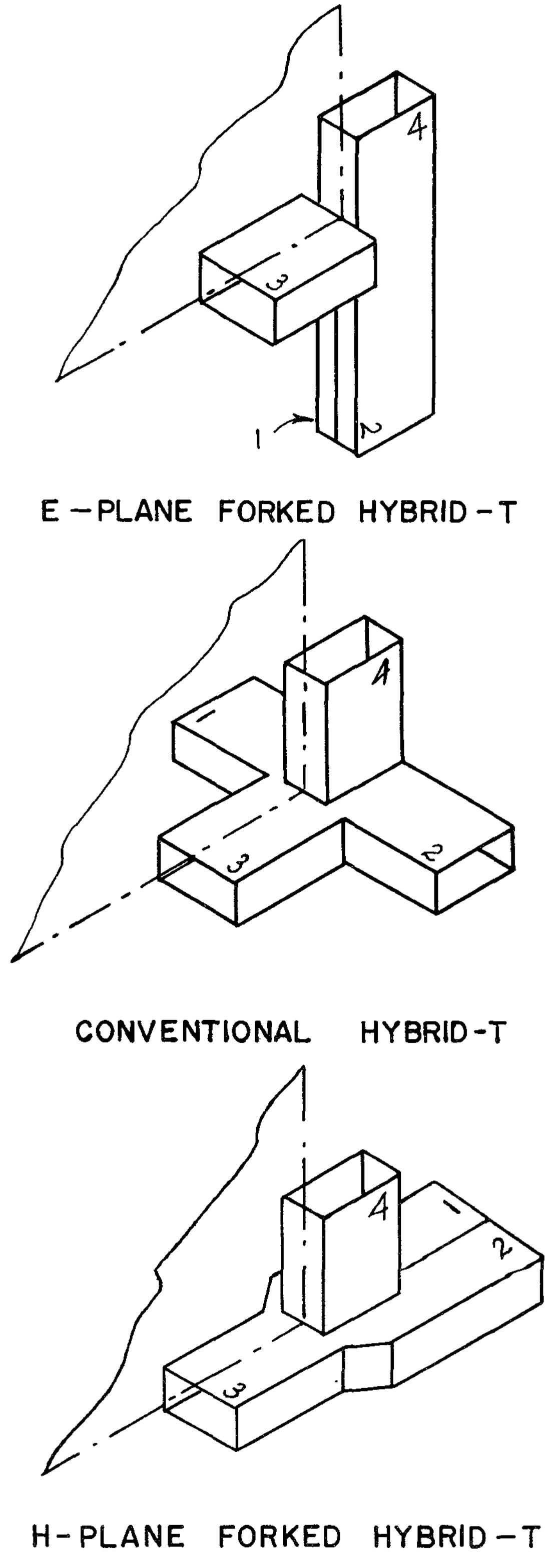

Fig. 1—Hybrid T with one symmetry plane.

* The essentials of this paper were submitted by the author as a thesis for the M.E.E. degree at the Polytechnic Institute of Brooklyn, Brooklyn, N. Y., at which time he was employed at Wheeler Laboratories, Inc., Great Neck, N. Y.

† Microwave Research Institute, Polytechnic Institute of Brooklyn, Brooklyn, N. Y.

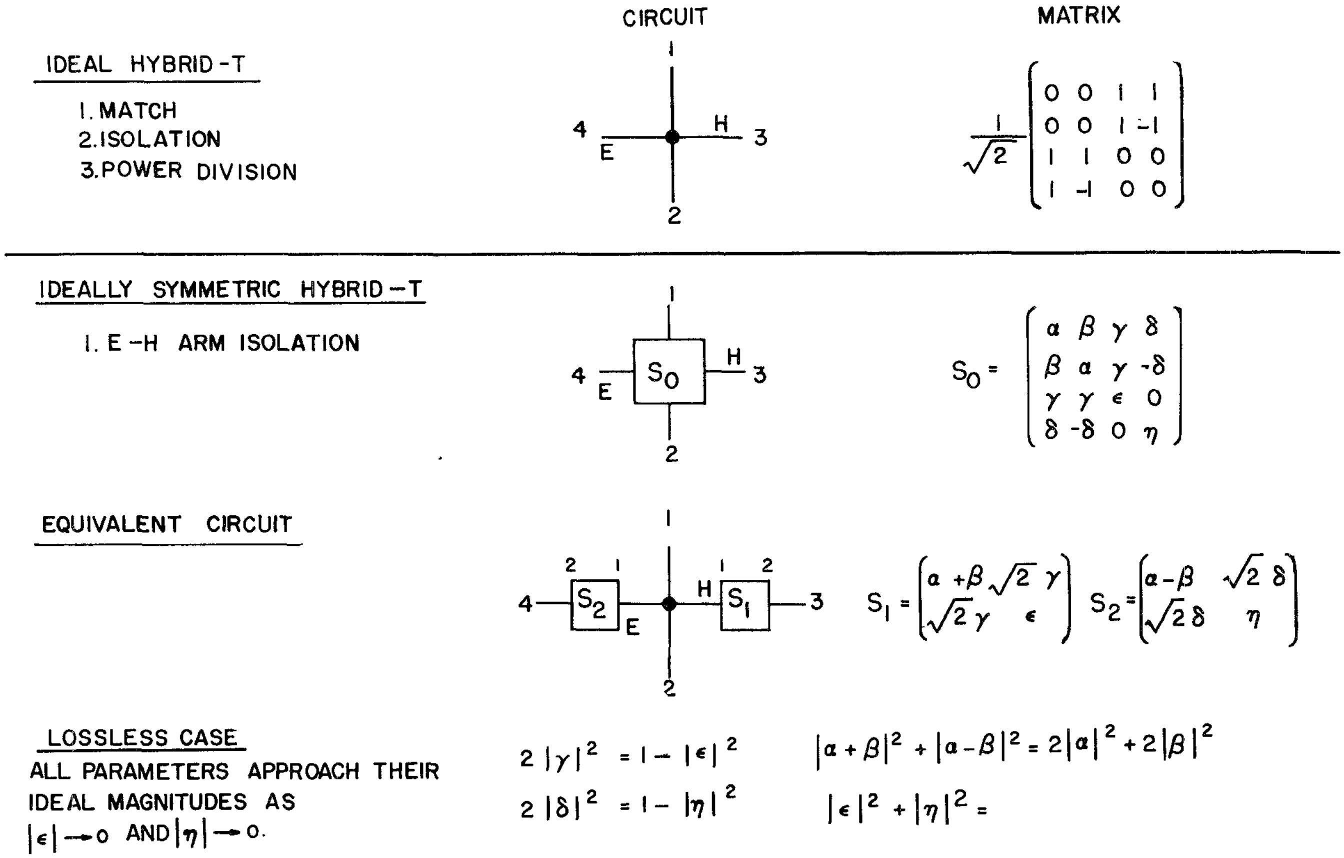

Fig. 2—Scattering relations for hybrid T.

respectively, from their relation to the corresponding three-port T structures evident in the conventional form of the hybrid-T. The H-plane forked hybrid-T[1] may be obtained from the conventional hybrid-T by folding the symmetrical arms back so that their now distinct center lines are parallel to that of the H-arm. The E-plane forked hybrid-T may be obtained by similarly folding the symmetrical arms down so that their now distinct centerlines are parallel to that of the E-arm; in addition, the symmetrical arms have been reduced to half their former height. The E-plane forked hybrid-T is related to the tapered branch and coaxial form of Lewis and Tillotson,[2] and that considered by Oguchi and Noda.[3]

General Properties of Hybrid-T Junctions

The essential properties of hybrid-T junctions may be reviewed with the aid of Fig. 2. The ideal hybrid-T is conventionally schematized, as shown at the top. Its properties are concisely summarized by the (normalized) scattering matrix to the right: it is a lossless reciprocal four-port; each port is matched to its transmission line; opposite ports (in the schematic) are isolated from one another; power entering any port divides evenly between the two adjacent ports.

Approaching this ideal performance over an appreciable range of frequencies with a particular junction of four waveguides is generally a difficult design problem. The first step in this direction is the specification of the symmetry which was noted in structures already considered. Carrying out the symmetry analysis indicated by Dicke[4] in slightly greater detail, one obtains the scattering matrix S_0 for the ideally symmetric hybrid-T junction. The zeroes which appear in this matrix demonstrate that the isolation between the H and E-arms of the junction follow automatically from this symmetry.

Above, symmetry has been applied to obtain relations (in addition to reciprocity) between the elements of the scattering matrix S_0. The same symmetry relations are

[1] P. A. Loth, Wheeler Laboratories Report 443, 1950.

[2] W. D. Lewis and L. C. Tillotson, "A non-reflecting branching filter for microwaves," *Bell Sys. Tech. Jour.*, vol. 27, pp. 84–95; January, 1948.

[3] B. Oguchi and K. Noda, Japanese Pat. No. 27-954, 1952. (This reference has only recently come to the author's attention.)

[4] C. G. Montgomery, R. H. Dicke, and E. M. Purcell, "Principles of Microwave Circuits," McGraw-Hill Book Co., Inc., New York, pp. 453–454; 1948.

equivalently, but more simply and physically, expressed by means of the equivalent circuit which shows the ideally symmetric hybrid-T to be composed of an ideal hybrid-T (transformers) and two *two-ports* located in the H and E arms of the hybrid. The scattering matrices of these two-ports are given in terms of the elements of S_0. Now, all the well-known results for two-ports become available. For example, when the junction is lossless, S_1 and S_2 are lossless and hence only $3+3=6$ real numbers in the complex elements α through η are independent. Further, the equations below the circuit diagram follow by inspection. The important quantitative conclusion to be drawn from these equations is that *the departure of the magnitude of every element in scattering matrix S_0 from its ideal value is bounded by the magnitudes of the H- and E-arm reflections* $|\epsilon|$ *and* $|\eta|$. The problem of designing a hybrid-T junction has been reduced to that of maintaining symmetry and simultaneously eliminating the H- and E-arm reflections.

The last implication of symmetry which it will be necessary to note explicitly is that a thin "magnetic conductor" in the symmetry plane or a thin electric conductor again in the symmetry plane does *not* affect, respectively, fields incident from the H or the E-arm.[5] Stated positively, in terms of the equivalent circuit of the ideally symmetric hybrid-T: a thin "magnetic conductor" in the symmetry plane affects only the two-port S_2, and a thin electric conductor, only the two-port S_1. The essential advantage of the E-plane forked hybrid-T is that, for E-arm incidence, the junction appears essentially as an E-plane bifurcation which produces relatively slight disturbance of the dominant mode fields, i.e., inherent broad-band match. This *eliminates* the need for a (fictitious) magnetic conductor. The difficult transition from the H-arm to the symmetrical arms may be matched by means of the electric conductor which is already available inside the junction, *i.e.*, the bifurcating element or center partition.

On the basis of the foregoing general considerations the following program was adopted for the experimental hybrid-T:

1. Reduce the inherently small E-arm reflection by means of some trimmer adjustment.
2. Reduce the H-arm reflection solely by shaping the center partition.

The Test Fixture

The design of the text fixture for the experimental E-plane forked hybrid was guided by the general approach to the electrical design indicated; that is, the design was directed towards a simple structure attaining the greatest measure of freedom in those adjustments affecting the H-arm reflection. The basic waveguide employed was 1.122×0.497 inside diameter rectangular waveguide (the larger X-band guide was chosen for higher power capacity), and the material was brass. Briefly, the proposed hybrid junction was cut along the plane of symmetry into two parts, mirror images of one another. These major halves were again divided into, essentially, E-arm and H-arm parts. The whole was assembled about a center partition which extended over the entire junction, Figs. 3 and 4.

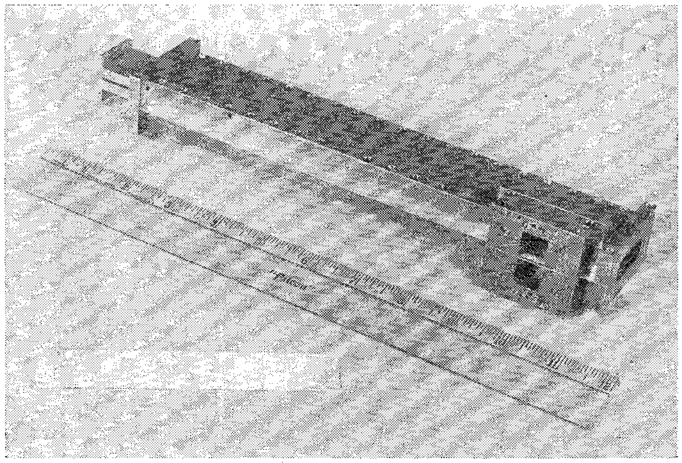

Fig. 3—E plane forked hybrid T test fixture.

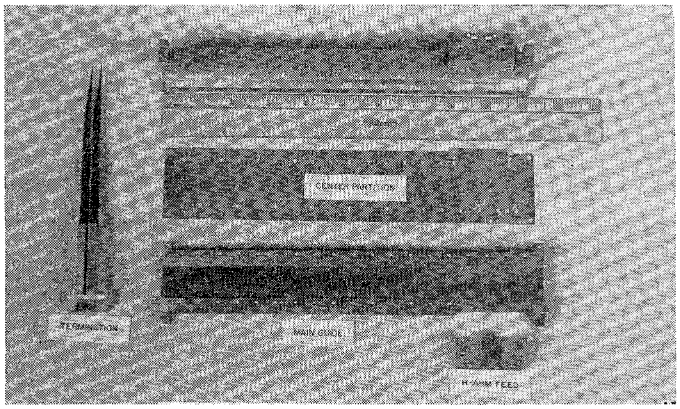

Fig. 4—E plane forked hybrid T test fixture, disassembled.

The center partition was cut from 0.020 sheet brass. It was designed as an expendable unit in that it may be simply reproduced from a master blank, removed, modified and/or replaced. As the blank extends over the entire junction, the problem of piecing together sections of partition and providing good electrical contact between thin sheets along their narrow dimension was avoided altogether; any arrangement could be cut in one piece.

The H-arm coupling was made as a subassembly so that this structure could also be varied, but this possibility will not be involved in work reported here.

[5] *Ibid.*, Ref. 4.

The entire assembly was held together by screws placed about 0.5-inch (center to center) apart. This spacing was chosen so as to be less than one-half wavelength (0.615 at 9.6 kmc), in order to preclude the possibility of resonant lengths of imperfect contact along abutting surfaces.

Tolerances on the waveguide dimensions 1.122 and 0.497 were held to ± 0.002 inch, exclusive of the variation in the thickness of the center partition. This variation is estimated to be less than ± 0.0015 inch.

All parts were pinned to insure reproducible assembly.

E-Arm Match, Experimental Hybrid-T

The reflection from the *E*-arm port of the empty hybrid (test fixture without matching elements) arises from two discontinuities:

1. The edge of the bifurcating element or partition.
2. The opening in one side wall which is necessary to admit the *H*-arm.

To emphasize the previously mentioned inherent *E*-arm match, ideal (broadband) methods for reducing each of these two sources of reflection to an arbitrary degree will be cited. The partition may be tapered to a fine edge, while the *H*-arm opening might be reduced to a small aperture. Such reduction of the *H*-arm would not be practical from the standpoint of subsequently matching the *H*-arm over an appreciable frequency range. However, the same effect may be obtained by introducing a set of thin conducting strips placed so as to conduct the dominant mode *E*-arm wall currents and be orthogonal to, and therefore only slightly disturb, the electric field incident from the *H*-arm (Fig. 5). The method actually employed to match the *H*-arm did not permit utilization of this approach.

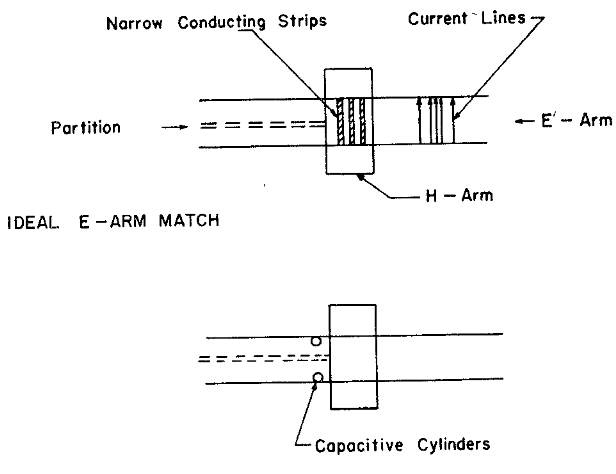

Fig. 5—*E* arm match.

The first step in the electrical design was a measurement of the *E*-arm reflection of the unmodified or empty hybrid-T. The result of this measurement is presented as a frequency contour in the reflection-coefficient plane,[6] Fig. 6. This reflection is seen to be less than 2.8 db SWR. The reference plane is at the flange of the test fixture.

Several types of matching elements were considered to reduce this reflection.[7] A set of capacitive cylinders[8] were chosen as an expedient to avoid the necessity for further machining operations at this stage. Such cylinders reduce the power capacity of the guide in which they are placed by 8 db.[9] For this reason it was recognized that the cylinder should be replaced at the developmental stage. When two 0.075-inch diameter cylinders are placed as shown in Fig. 5, the *E*-arm reflection is reduced to less than 0.8-db SWR, as shown by the designated contour in Fig. 6.

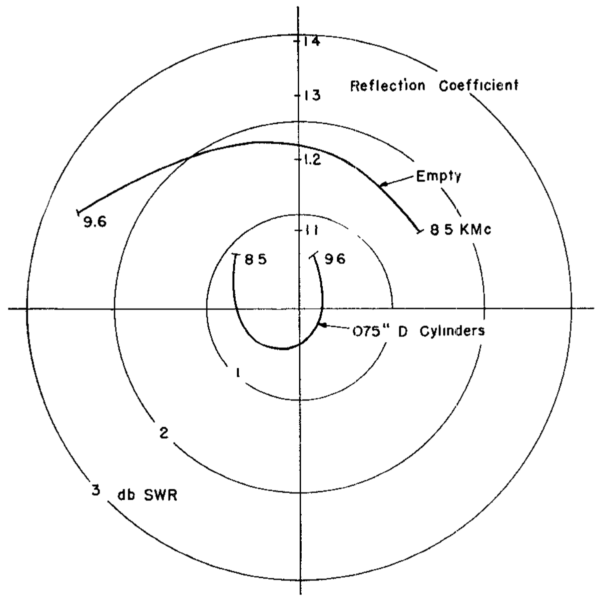

Fig. 6—*E* arm match, reflection coefficient plane.

H-Arm Match, Experimental Hybrid-T

The starting point for consideration of the design of the *H*-arm matching elements was again a structure which might intuitively be called the empty junction. It corresponds to the structure shown in Fig. 7, with the center partition cut back still further so that it does not extend into the *H* arm, and that its leading edge coincides with the left side of the *H*-arm opening. The experimental partition for this condition is number 1 in

[6] H. A. Wheeler, "Wheeler Monographs," vol. I, Wheeler Monograph 4, Wheeler Laboratories, Inc.; 1953.

[7] W. K. Kahn, "*E*-plane forked hybrid-T," M.E.E. Thesis, Polytechnic Institute of Brooklyn; June, 1954.

[8] N. Marcuvitz, "Waveguide Handbook," McGraw-Hill Book Co., Inc., New York, pp. 268–271; 1948.

[9] H. A. Wheeler, "Pulse Power Chart for Waveguides and Coaxial Lines," Wheeler Monograph 16, Wheeler Laboratories, Inc.; 1953.

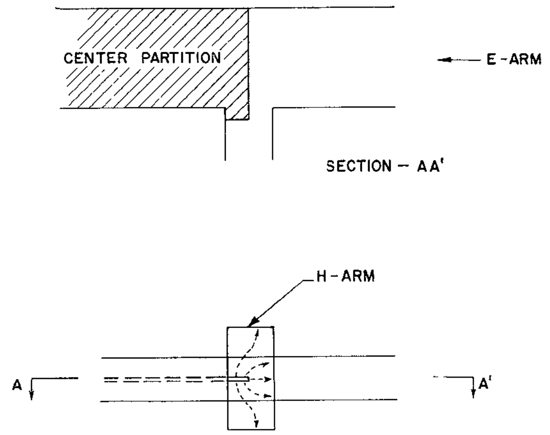

Fig. 7—*H* arm match (a).

Fig. 9. The reflection from this empty junction was extremely high, approximately 30-db SWR. The frequency contour with reference plane at the flange of the test fixture is shown on the reflection coefficient plane, Fig. 10. This reflection was to be reduced principally by adjustment of the center partition, *i.e.*, by independent *Y*-arm matching element inherent in junction.

No rigorous theoretical treatments directly applicable to this problem were known. Therefore, the procedure followed was to formulate some ideas of the behavior of the junction fields on the basis of approximate theory; these ideas then suggested general shapes of center partitions which would reduce the *H*-arm reflection. The appropriateness of these shapes was then checked and refined experimentally. The test fixture, it will be recalled, was specifically designed to facilitate this approach.

Consider, first of all, the dominant mode field which must be excited in the two symmetrical arms of the hybrid-T by the dominant mode fields incident from the *H*-arm. Each of these is a TE_{01} mode; the electric vectors in the symmetrical arms being oppositely directed. The planes of both the electric and magnetic vectors in these arms are perpendicular to the corresponding planes of the incident *H*-arm fields. Only the longitudinal *H*-arm magnetic fields couple with the transverse components of the symmetrical arm fields. In order to produce additional coupling by transverse components of incident electric and magnetic fields parallel to the desired symmetrical arm fields, some perturbing element may be inserted in the *H*-arm guide. The center partition may be cut so as to form an *H*-arm ridge which has this effect. Such a ridge is shown in Fig. 7, with the electric field lines sketched in.

The same perturbation is also suggested from another point of view. The intersection of the *H*- and *E*-arm guides forms a square coupling iris whose dimensions equal the narrow height of each waveguide. The TE_{01} fields incident from the *H*-arm are therefore cut off in this cross section. A well-known method of increasing the cutoff wavelength of a given rectangular waveguide is to insert a ridge parallel to the electric field.[10]

Finally, the magnetic coupling noted above is related to that occurring in a shunt T junction.[11] From this standpoint the *H*-arm sees the two symmetrical arms as parallel loads. The resulting impedance mismatch is 4:1, since each of the symmetrical arms is only one-half the height of the (normal) *H*-arm guide. Ridge loading has the effect of lowering the characteristic impedance of rectangular waveguide, and hence, a section of ridged guide may be utilized as a transformer.

The result inserting the ridge shown in Fig. 7 is illustrated by the designated frequency contour in Fig. 10. The impedance step from ridged to ordinary rectangular waveguide has not yet been positioned to obtain the favorable transformer action noted in the preceding paragraph. When this latter adjustment is made, the resultant reflection is less than 16-db SWR.

One further type of adjustment of the center partition would, in effect, provide a stub line for tuning the *H* arm of the hybrid-T. It arises as follows. Because of the symmetry of the hybrid-T junction, a wave incident from the *H*-arm does not excite the propagating polarization of the TE_{01} mode in the *E* arm. However, the orthogonal polarization is excited and would, except for the fact that it is below cutoff in the design range of frequencies, propagate up the *E*-arm of the junction. Again, ridge loading may be employed to permit a perturbed form of the TE_{01} mode to propagate. This is shown in Fig. 8,

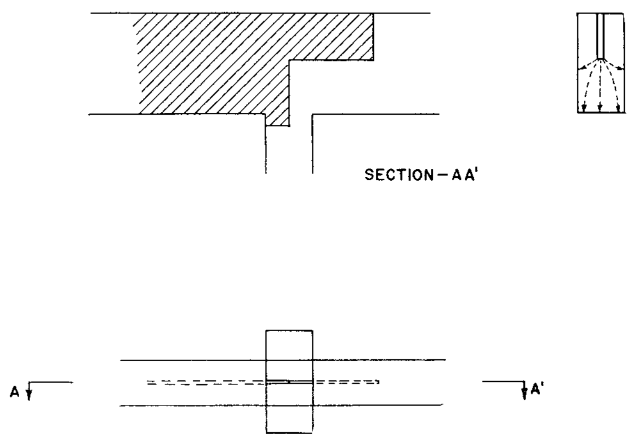

Fig. 8—*H* arm match (b).

where the electric field lines have been sketched in the side view (see experimental partitions numbers 2 and 3 in Fig. 9). The stub line may be tuned by varying the length of the ridge and its coupling to the *H* and symmetrical arms by varying its height. However, since the guide wavelength of the perturbed TE_{01} mode also de-

[10] *Ibid.*, Ref. 8, pp. 399–400.
[11] *Ibid.*, Ref. 4, pp. 294–295.

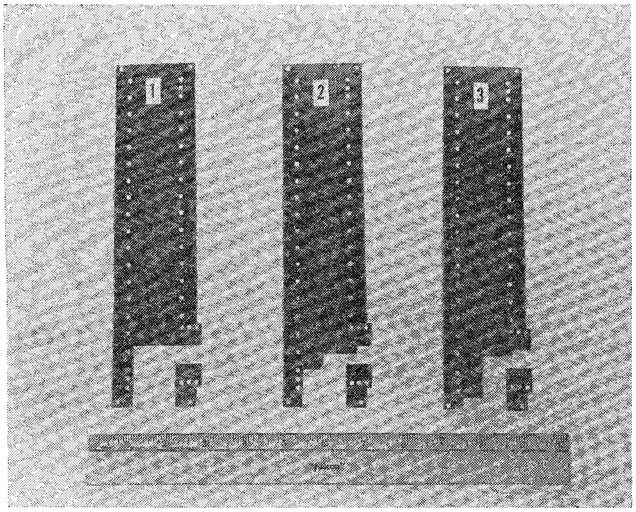

Fig. 9—Experimental partitions.

pends on the ridge height, these two adjustments are not entirely independent. The effect of the stub line is illustrated by the centered contour in Fig. 10. The maximum SWR in the design band is 2.6 db.

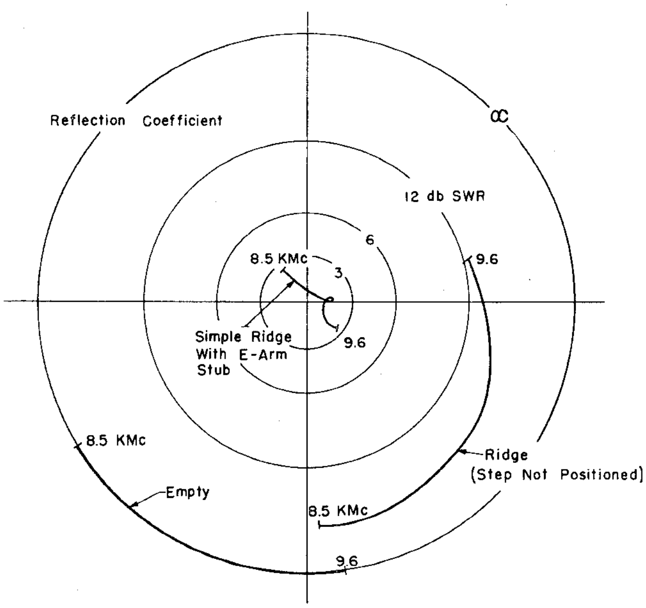

Fig. 10—*H* arm match.

Developmental Hybrid T

Considerable improvements were realized in modifying the basic elements of the experimental hybrid-T into the developmental form shown in Fig. 11. The inherent high pulse power capacity of the *E*-arm was restored by replacement of the capacitive cylinders a step in the symmetrical arm guide height (change of characteristic impedance). The *E*-arm match was further trimmed to within 0.6-db swr by the addition of a small inductive iris. In the *H*-arm, the center partition was extended to provide an additional transformer section and the internal dimensions of the partition slightly modified to

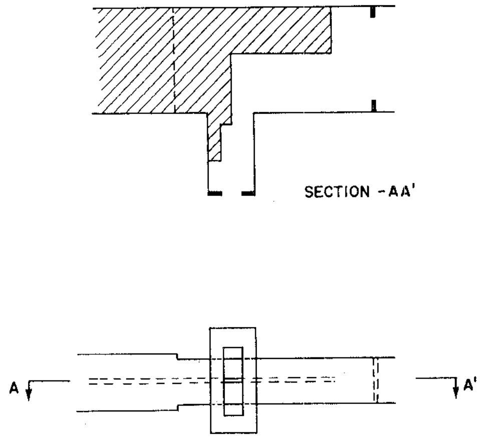

Fig. 11—*E* and *H* arm match with trimmer elements.

utilize this new degree of freedom. A low-*Q* resonant window was added at the *H*-arm port trimming the reflection to 0.8-db SWR. These results, plus bounds on remaining performance parameters which follow from equations at lower right of Fig. 2, are in Table I.

TABLE I

Performance of *E* plane forked hybrid *T*.
(Data supplied by Wheeler Labs., Inc., Great Neck, L. I.)

8.5 – 9.6 KMc	db SWR	VSWR
E – ARM REFLECTION	0.6	1.07
H – ARM REFLECTION	0.8	1.10
SYMMETRICAL ARM REFLECTION (CALC.)	<0.7	< 1.08
	db	
SYMMETRICAL ARM ISOLATION (CALC.)	> 28	
	Mw	
E – ARM POWER CAPACITY	>0.9	

Power Capacity

The pulse power capacity of the *E*-arm of the hybrid-T was regarded as inherently limited by the excess electric field intensity at the rounded leading edge of the center partition, over that obtaining in uniform waveguide. A calculation, based on a conformal mapping, was made to determine the order of magnitude of the excess gradient to be expected.

The conformal mapping is set forth in Fig. 12. At the top are the two planes connected by the transformation $w = z - \text{Ln } z$, where Ln z is the principal value of $\ln z$, $-\pi < \text{Im}(\ln z) \leq \pi$. The rounded edge, for which the polar equation is given, corresponds to the potential $v = 0$. The general equation for the equipotentials is given at the lower left. At the lower right an expression for the electric field along any equipotential is given. A construction of the locus of the electric vector for the edge ($v = 0$) is shown. In particular, the maximum excess gradient is cited.

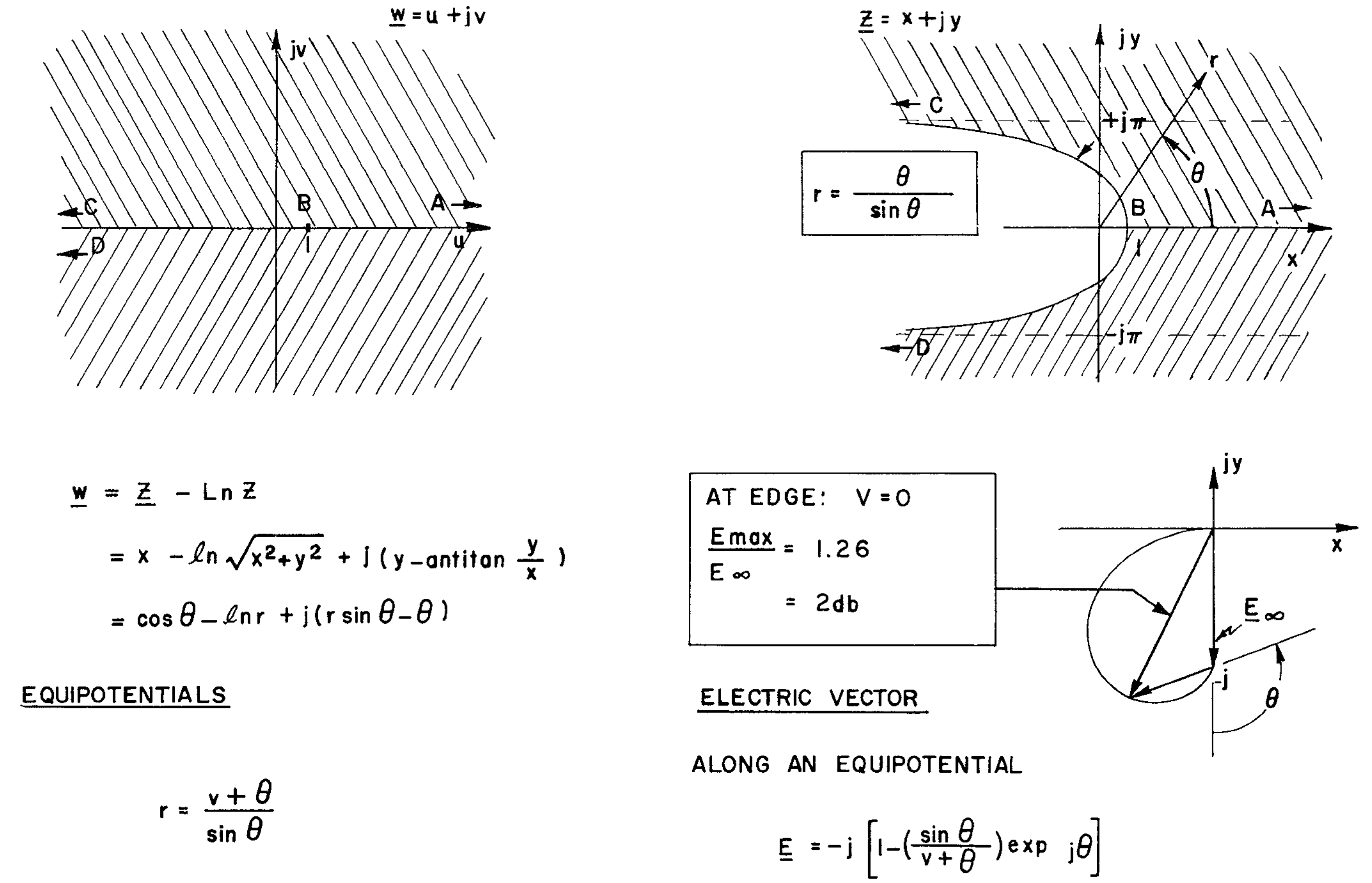

Fig. 12—Conformal mapping for calculation of the maximum gradient.

To facilitate comparison of the particular contour arising from this simple conformal map with edges encountered in practice, a profile is shown in Fig. 13.

ACKNOWLEDGMENT

The developmental E-plane forked hybrid T and the experimental results on E-arm power capacity are quoted by permission of H. A. Wheeler, President, Wheeler Laboratories, Inc., Great Neck, N. Y.

The author wishes to express his appreciation for the counsel of his thesis advisor, Dr. L. B. Felsen.

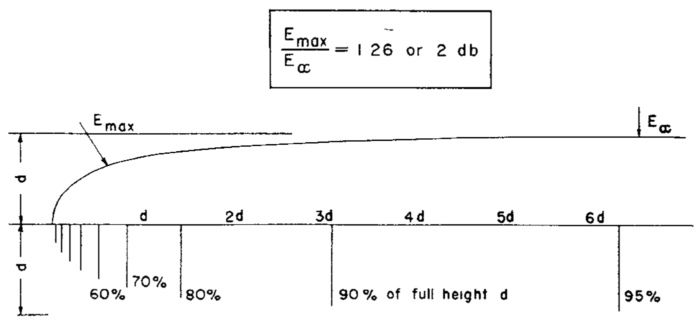

Fig. 13—Profile of contour.